

A new modified expanding cavity model for characterizing the spherical indentation behavior of bulk metallic glass with pile-up

K. Ai and L.H. Dai*

State Key Laboratory of Nonlinear Mechanics, Institute of Mechanics, Chinese Academy of Sciences, Beijing 100080, China

Received 2 October 2006; revised 11 December 2006; accepted 8 January 2007

Available online 6 February 2007

Spherical nanoindentation tests were performed on $\text{Zr}_{41.2}\text{Ti}_{13.8}\text{Cu}_{12.5}\text{Ni}_{10}\text{Be}_{22.5}$ bulk metallic glass and pile-ups were observed around the indenter. A new modified expanding cavity model was developed to characterize the indentation deformation behavior of strain-hardening and pressure-dependent materials. By using this model, the representative stress–strain response of this bulk metallic glass to hardness and indentation in the elastic–plastic regime were obtained taking into consideration the effect of pile-up. © 2007 Acta Materialia Inc. Published by Elsevier Ltd. All rights reserved.

Keywords: Expanding cavity model; Pile-up; Bulk metallic glass; Hardness; Stress–strain

Considerable efforts have been devoted to studying the inhomogeneous deformation and fracture behavior of bulk metallic glasses (BMGs) [1,2]. Recent investigation showed that the shear fracture of BMGs does not occur along the maximum shear stress plane, irrespective of whether the loading is compressive or tensile [3]. Therefore, the Mohr–Coulomb (MC) and Drucker–Prager (DP) criteria were suggested to characterize the yield behavior of BMGs [4–6]. In addition, a depth-sensing indentation technique has proved to be a powerful tool for investigating material properties such as hardness, elastic modulus, stress–strain response, etc. [7,8]. Increasing efforts have been made recently to use this technique to study the deformation behavior of BMGs [9–14]. Theoretical analyses employing various models have been proposed to explain the elasto-plastic properties of materials undergoing indentation testing, among which the expanding cavity model (ECM) developed by Johnson [15] is particularly valuable. Using the DP yield criterion, Narasimhan [16] developed a modified expanding cavity model (DP-ECM) to describe the indentation deformation of pressure-dependent materials. In this model, the strain-hardening effect was not included. Recently, two new modified ECMs for elastic power-law hardening and linear-hardening materials were developed by Gao

et al. [17]. However, these two strain-hardening-based models are confined to pressure-independent materials. Furthermore, for some materials pile-ups around the indenter are usually observed and neglecting the pile-up effect may lead to errors in evaluating hardness and stress–strain response [8]. Ahn and Kwon [18] proposed a hardening exponent iterative method to take account of the effect of pile-up, but in their work only the fully plastic response was considered. In the present study, spherical nanoindentation tests were performed on $\text{Zr}_{41.2}\text{Ti}_{13.8}\text{Cu}_{12.5}\text{Ni}_{10}\text{Be}_{22.5}$ BMG and pile-ups around the indenter were observed. A new modified ECM was developed to characterize the indentation deformation behavior of strain-hardening and pressure-dependent materials. By using this model and an iterative method, the representative stress–strain response of this BMG to hardness and indentation in the elastic–plastic regime were obtained with pile-up.

The test material $\text{Zr}_{41.2}\text{Ti}_{13.8}\text{Cu}_{12.5}\text{Ni}_{10}\text{Be}_{22.5}$ BMG was fabricated by the same routine as used by Liu et al. [19]. The specimens were then machined into disks 8 mm in diameter and 1 mm thick and the top surfaces of the specimens were electro-polished in methanol solution containing 33 vol.% HNO_3 . A MTS Nano Indenter XP with a spherical diamond indenter of 10.6 μm in radius was used to perform the nanoindentation tests. All tests were performed in load-control mode using a loading rate of 1 mN s^{-1} . Single loading–unloading experiments of peak load 10, 15, 25, 30, 90, 150, 200, 300, 400, 500 mN were performed. In addition, the final peak

* Corresponding author. Tel.: +86 10 62616852; fax: +86 10 62579511; e-mail: lhだい@lnm.imech.ac.cn

load was 512 mN and seven partial unloadings down to 90% of peak load at each point were also applied. For each loading case, more than six indentations were performed to determine reproducibility. A typical load–displacement curve and the atomic force microscope (AFM) image of the residual indent at 500 mN are shown in Figure 1. Figure 1b clearly shows pile-up around the indenter. In addition, the heights of the pile-ups for relatively larger loading cases were also measured using the AFM.

The stress, strain and displacement fields prevailing in a hollow sphere with inner radius a and outer radius b , subjected to the internal pressure p , are considered. The radius of the elastic–plastic interface is c and the pressure acting on this interface is p_c . The linear DP yield criterion in spherical coordinates $(\sigma_r, \sigma_\theta, \sigma_\phi)$ is represented by [20]:

$$(\sigma_\theta - \sigma_r) + (\sigma_r + 2\sigma_\theta) \tan \alpha/3 = (1 - \tan \alpha/3)\sigma_y, \quad (1a, b)$$

where α is the pressure sensitivity index and σ_y is the uniaxial compressive yield stress. Based on the solution of a strain-hardening material with von Mises' yield criterion reported by Gao et al. [17], the basic equations for determining the elasto-plastic ($a \leq r < c$) solution of the power-law hardening and pressure-dependent materials are:

$$\sigma_\theta - \sigma_r = r d\sigma_r / (2dr), \quad \sigma_e = K \varepsilon_e^n, \quad (1a, b)$$

$$\varepsilon_\theta = \varepsilon_\phi = (\sigma_\theta - \sigma_r) \varepsilon_e / (2\sigma_e), \quad (2a, b)$$

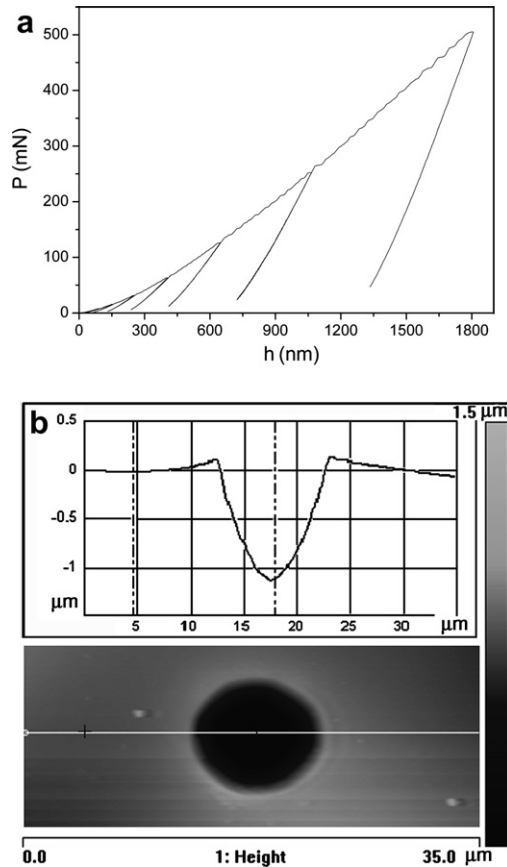


Figure 1. (a) A typical load–displacement curve and (b) AFM image of the residual indent at 500 mN.

$$\varepsilon_r = -(\sigma_\theta - \sigma_r) \varepsilon_e / \sigma_e, \quad (2c)$$

$$\sigma_e = \sigma_\theta - \sigma_r, \quad r d\varepsilon_\theta / dr = \varepsilon_r - \varepsilon_\theta, \quad (3a, b)$$

where E is the Young's modulus, K is a material constant ($K = E^n / \sigma_y^{n-1}$), and σ_e and ε_e are equivalent stress and strain, respectively. The boundary conditions are:

$$\sigma_r|_{r=a} = -p, \quad \sigma_r|_{r=c} = -p_c, \quad (4a, b)$$

$$(\sigma_\theta - \sigma_r) + (\sigma_r + 2\sigma_\theta) \tan \alpha/3 = (1 - \tan \alpha/3)\sigma_y|_{r=c}. \quad (4c)$$

It should be noted that the influence of the hydrostatic stress on the plastic strain increment was ignored in deriving Eq. (2a,b,c) to obtain the analytic solution, and the relative error of doing this will be discussed below.

According to the continuity of σ_r at $r = c$, the pressure acting on elastic–plastic interface p_c will be given by [16]

$$P_c = -\sigma_r|_{r=c} = -\frac{(1 - \tan \alpha/3)\sigma_y}{[3b^3/(2c^3) + \tan \alpha]}(1 - b^3/r^3), \quad (5)$$

which can be used in actual indentation tests as $b \rightarrow \infty$ to obtain $p_c = 2(1 - \tan \alpha/3)\sigma_y/3$. Solving this boundary-value problem then leads to

$$\sigma_r = -(2/3)(1 - \tan \alpha/3)\sigma_y\{1 + [(c/r)^{3n} - 1]/n\}, \quad (6a)$$

$$\sigma_\theta = \sigma_\phi = (1 - \tan \alpha/3)\sigma_y[(1 - 2/3n)(c/r)^{3n} + (2/3)(1/n - 1)], \quad (6b)$$

$$u_r = \sigma_y(1 - \tan \alpha/3)^{1/n} c^3 / (2Er^2). \quad (6c)$$

Using Eq. (6a) in boundary condition Eq. (4a) gives

$$p/\sigma_y = (2/3)(1 - \tan \alpha/3)\{1 + [(c/a)^{3n} - 1]/n\}. \quad (7)$$

Comparing the ratio of p/σ_y in Eq. (7) with the result of Narasimhan [16], in which the hydrostatic stress on plastic strain increment was considered in the perfect-plasticity case, the relative error obtained is <13.6%, as $c/a = 2, 0 \leq \alpha \leq 20^\circ$. Choosing $\alpha = 10.3^\circ$ (mentioned later) for the $\text{Zr}_{41.2}\text{Ti}_{13.8}\text{Cu}_{12.5}\text{Ni}_{10}\text{Be}_{22.5}$ BMG used in present study gives a relative error was 7.6%. According to this comparison, it is acceptable to ignore the hydrostatic stress on the plastic strain increment.

According to Johnson [15], the volume of the material displaced by the indenter is accommodated by the radial expansion of the hemispherical core:

$$2\pi a^2 du_r(a) = \pi a^2 \tan \beta da \cong \pi a^2 (a/R) da,$$

where β is the contact angle between the indenter and the specimen, and R is the indenter radius, as shown in Figure 2. Then, the plastic zone radius c and contact radius a is obtained by using $c \rightarrow 0$ as $a \rightarrow 0$:

$$c^3/a^3 = Ea(1 - \tan \alpha/3)^{-1/n} / (4\sigma_y R).$$

However, the stress state immediately beneath the indenter will not be purely hydrostatic in actual indentation tests. Employing the modification idea used in Studman et al. [21], the new modified expanding cavity model (n -DP-ECM) for strain-hardening and pressure sensitivity materials was obtained as:

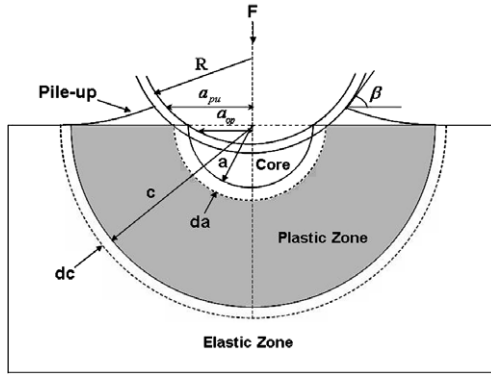


Figure 2. Schematic illustrating elastic-plastic indentation as idealized by the expanding cavity model considering pile-up.

$$\frac{H}{\sigma_y} = \frac{2}{3} \left[(1 - 1/n)(1 - \tan \alpha/3) + (1/n + 3/4)(Ea/4R\sigma_y)^n \right]. \quad (8)$$

It is interesting to find that Eq. (8) can be reduced to

$$\frac{H}{\sigma_y} = \frac{2}{3} \left[(1 - 1/n) + (1/n + 3/4)(Ea/4R\sigma_y)^n \right], \quad \text{as } \alpha = 0$$

and

$$\frac{H}{\sigma_y} = \frac{2}{3} \left[7/4 + \ln(Ea/4R\sigma_y) \right], \quad \text{as } \alpha = 0, \quad n \rightarrow 0.$$

These two results were the same as those obtained previously by Gao et al. [17].

The spherical indentation deformation of $\text{Zr}_{41.2}\text{Ti}_{13.8}\text{Cu}_{12.5}\text{Ni}_{10}\text{Be}_{22.5}$ is geometrically modeled in Figure 2, where material pile-up around the indenter is included. According to Ahn and Kwon [18], a_{op} is the contact radius without piling-up defined by the Oliver–Pharr (OP) method [7] and a_{pu} is the real contact radius. To calculate the real contact radius, the strain-hardening-dependent relationship $a_{pu}^2 = (5 - 3n^{0.7})a_{op}^2/4$ proposed by Taljat and Zacharia [22] based on the finite element simulation under a J_2 -associated flow rule, a ratio a/R of 0.5, a friction coefficient of 0.2 and a ratio σ_y/E of 1/500 was used in present study. In spite of the difference in material parameters, a good consistency was obtained between the depths of piling-up calculated by the formulation of Taljat and Zacharia [22] and the results of AFM, and the average relative error was less than 9.6%. According to the uniaxial compression test [19], the pressure sensitivity index α is approximately equivalent to 10.3° [20]. E and σ_y values of 95 and 1.71 GPa, respectively, are obtained, and these values will be used in the calculations below.

Both the results of normalized hardness H/σ_y with normalized indentation strain $Ea/\sigma_y R$ in the present study and Patnaik et al.'s [11] work by OP analysis are shown in Figure 3. For comparison, the results based on the pile-up heights measured using AFM are also shown in Figure 3. It is noted that both the results obtained by OP analysis deviate from the results of AFM. According to the definition of hardness $H = F/\pi a_{op}^2$, this deviation is chiefly due to the contact radius a_{op} , which is smaller than the real contact radius a_{pu} . Also, a similar deviation in indentation representative stress-strain relation was found between the results

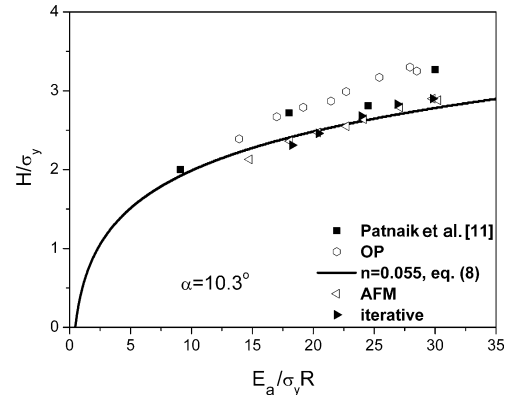


Figure 3. Variation of normalized hardness with normalized indentation strain.

of present study by OP analysis and the uniaxial compression test for the same BMG [19] as shown in Figure 4. We conclude from these observations that the pile-up effect cannot be ignored in evaluating the hardness and the stress-strain response of BMGs. Therefore, the hardening exponent iterative procedure was employed below to consider the effect of pile-up.

Ignoring the influence of the shear bands during indentation and assuming the strain-hardening of $\text{Zr}_{41.2}\text{Ti}_{13.8}\text{Cu}_{12.5}\text{Ni}_{10}\text{Be}_{22.5}$ BMG to be isotropic, the indentation representative stress-strain ($\sigma_R - \varepsilon_R$) can be represented by

$$\sigma_R = \begin{cases} E\varepsilon_R, & \varepsilon_R \leq \sigma_y/E \\ K\varepsilon_R^n, & \varepsilon_R > \sigma_y/E \end{cases} \quad (9)$$

Following the pioneering study by Tabor [23], the indentation representative stress σ_R can be obtained from the mean contact pressure H as

$$\frac{H}{\sigma_R} = C(\varepsilon_R) = \frac{2}{3} \left[(1 - 1/n)(1 - \tan \alpha/3) + (1/n + 3/4)(Ea/4R\sigma_y)^n \right], \quad (10)$$

where C is a function of the indentation representative strain ε_R for a given material. According to Ahn and Kwon [18], $\varepsilon_R = 0.1 \tan \beta \approx 0.1a/R$. The boundary between the elastic-plastic regime and the fully plastic regime is determined by normalized indentation strain $Ea/\sigma_y R$, and the value of $Ea/\sigma_y R$ is approximately 40

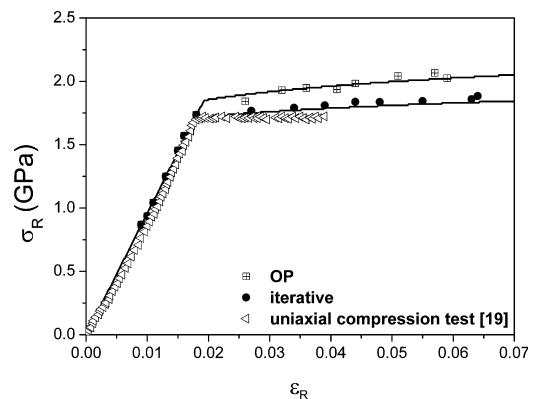


Figure 4. Comparisons between flow properties calculated from the spherical indentation test and that from the uniaxial compression test.

[24]. In the present study, all the values of $Ea/\sigma_y R$ were calculated to be < 40 as shown in Figure 3. Therefore, the material is in the elastic–plastic regime under indentation. Taking the initial value of the strain-hardening exponent n to be 0.1, the value of n was modified in the iterative calculation using the stress–strain equation $\sigma_R = k\epsilon_R^n$ until the input value equalled the returned value. Then, the final value of n was achieved.

The iterative results of normalized hardness H/σ_y with normalized indentation strain $Ea/\sigma_y R$ are shown in Figure 3. It can be observed in Figure 3 that the iterative results agree well with the AFM results. In addition, the final average iterative n is obtained as 0.055. Submitting this value and $\alpha = 10.3^\circ$ into Eq. (8), the n -DP-ECM curve is also obtained in Figure 3. As be observed, the trend predicted by the n -DP-ECM model follows closely both the results of the iterative method and AFM, thereby supporting the new model. Furthermore, the results of indentation representative stress–strain relation by the iterative method and OP analysis are shown in Figure 4, respectively. It can be seen that the iterative results are in a good agreement with the uniaxial compression data and the assumption of incompressibility may be responsible for the slight deviation. These comparisons demonstrate that our new n -DP-ECM model is satisfactory for evaluating the hardness and stress–strain response of BMGs considering the effect of pile-up.

In summary, spherical nanoindentation tests were employed to characterize the hardness and indentation representative stress–strain of $\text{Zr}_{41.2}\text{Ti}_{13.8}\text{Cu}_{12.5}\text{Ni}_{10}\text{Be}_{22.5}\text{BM}$. By using the new modified n -DP-ECM model and the iterative method, the hardness and indentation representative stress–strain of this BMG in the elastic–plastic regime were obtained, taking into consideration the effect of pile-up. As a result, the iterative hardness agreed well with the AFM results. Excellent agreement was also obtained between the iterative results of indentation representative stress–strain and the uniaxial compression tests.

This work is supported by the National Natural Science Foundation of China through Grant Nos.

10472119 and 10232040; the key project of Chinese Academy of Sciences through KJCX-SW-L08. L.H. also gratefully acknowledges the support of the K.C. Wong Education Foundation, Hong Kong.

- [1] F. Spaepen, *Acta Metall.* 25 (1977) 407.
- [2] T.C. Hufnagel, P. El-Deiry, R.P. Vinci, *Scripta Mater.* 43 (2000) 1071.
- [3] Z.F. Zhang, J. Eckert, L. Schultz, *Acta Mater.* 51 (2003) 1167.
- [4] P.E. Donovan, *Acta Metall.* 37 (1989) 445.
- [5] R. Vaidyanathan, M. Dao, G. Ravichandran, S. Suresh, *Acta Mater.* 49 (2001) 3781.
- [6] M. Martin, N.N. Thadhani, L. Kecskes, R. Dowding, *Scripta Mater.* 55 (2006) 1019.
- [7] W.C. Oliver, G.M. Pharr, *J. Mater. Res.* 7 (1992) 1564.
- [8] Y.T. Cheng, C.M. Cheng, *Mater. Sci. Eng. R* 44 (2004) 91.
- [9] C.A. Schuh, T.G. Nieh, *Acta Mater.* 51 (2003) 87.
- [10] W.H. Jiang, M. Atzmon, *J. Mater. Res.* 18 (2003) 755.
- [11] M.N.M. Patnaik, R. Narasimhan, U. Ramamurty, *Acta Mater.* 52 (2004) 3335.
- [12] H.W. Zhang, X.N. Jing, G. Subhash, L.J. Kecskes, R.J. Dowding, *Acta Mater.* 53 (2005) 3849.
- [13] G.R. Trichy, R.O. Scattergood, C.C. Koch, K.L. Murty, *Scripta Mater.* 53 (2005) 1461.
- [14] B. Yang, R. Laura, T.G. Nieh, *Scripta Mater.* 54 (2006) 1277.
- [15] K.L. Johnson, *J. Mech. Phys. Solids* 18 (1970) 115.
- [16] R. Narasimhan, *Mech. Mater.* 36 (2004) 633.
- [17] X.L. Gao, X.N. Jing, G. Subhash, *Int. J. Solids Struct.* 43 (2006) 2193.
- [18] J.H. Ahn, D. Kwon, *J. Mater. Res.* 16 (2001) 3170.
- [19] L.F. Liu, L.H. Dai, Y.L. Bai, B.C. Wei, J. Eckert, *Mater. Chem. Phys.* 93 (2005) 174.
- [20] W.F. Chen, D.J. Han, *Plasticity for Structural Engineers*, Springer Verlag, Berlin, 1988.
- [21] C.J. Studman, M.A. Moore, S.E. Jones, *J. Phys. D Appl. Phys.* 10 (1977) 949.
- [22] B. Taljat, T. Zacharia, *Int. J. Solids Struct.* 35 (1998) 4411.
- [23] D. Tabor, *Hardness of Metals*, Clarendon Press, Oxford, 1951.
- [24] K.L. Johnson, *Contact Mechanics*, Cambridge University Press, Cambridge, 1985.